Interatomic potential for silicon clusters, crystals, and surfaces

Barry C. Bolding and Hans C. Andersen
Department of Chemistry, Stanford University, Stanford, California 94305
(Received 28 August 1989)

We have developed an interatomic potential suitable for the modeling of silicon in a wide range of bonding environments. The potential is of the general form developed by Tersoff, with the interaction between a pair of atoms being dependent on the environment of the pair. The atom-atom potential-energy function is expressed as a sum of π- and σ-bonding terms, each independently influenced by the environment. The functional form of the potential and the parameters in the potential were chosen to fit a variety of data on silicon, including the structure and energy of small clusters of 2–10 atoms, the crystal structures, the elastic constants of the diamond-lattice phase, and some surface properties. We present the results of using this potential to model small clusters (2–10 atoms), crystal phases, point defects in the diamond lattice, the 2×1 reconstructions of the Si(100) and Si(111) surfaces, and the 7×7 reconstruction of Si(111). Our present potential is compared in detail to other potentials that have been developed to model the properties of silicon.

I. INTRODUCTION

For obvious technological reasons a great deal of theoretical research effort has recently been directed toward the study of the structure of atomic arrangements in systems made up of silicon. The research effort has attacked these problems from several different directions.

Large-scale *ab initio* calculations for silicon clusters of up to ten atoms have recently been performed.[1–7] These have provided insight into how the bonding in silicon changes as the clusters grow larger. It has been found, for this number of atoms, that compact structures with many strained bonds are more stable than crystal fragments that have fewer bonds. Hohenberg-Kohn density-functional-theory (DFT) quantum calculations using the Kohn-Sham local-density approximation (LDA) have qualitatively supported these results and even allowed some dynamical and temperature-dependent properties to be studied.[8] Some authors have attempted to use semiempirical quantum calculations to make order-of-magnitude predictions of the cluster sizes at which the low-coordination-number diamond fragments become more stable than close-packed structures.[9,10]

Another approach to the theoretical study of silicon has been the use of interatomic potential functions to model bulk and surface properties. Such functions typically have interactions among pairs and triplets of atoms (or more complicated terms) and incorporate a number of adjustable parameters. A set of theoretical and experimental data is then used as a data base for choosing the parameters in the potential. This approach was first used for silicon by Keating,[11] but his potential was applicable only for small distortions about the equilibrium diamond lattice. The first silicon potentials applicable to all interatomic distances were developed by Pearson, Takai, Halicioglu, and Tiller (PTHT) (Refs. 12 and 13) and later by Stillinger and Weber (SW).[14] These authors knew that simple two-body potentials, typically used in molecular-dynamics simulations, would be inadequate in producing the diamond crystal structure and the random tetrahedral network structure of the amorphous solid. They formulated simple three-body terms that stabilized the diamond structure. The SW potential adequately modeled the structure of both the crystalline and liquid phases. Subsequently, other authors applied the SW potential to a wide range of systems, including surfaces,[15,16] clusters,[17–19] and point defects in crystals.[15] These calculations have shown the SW potential to be useful for qualitative studies, but it provides an inadequate description of undercoordinated or overcoordinated silicon. The PTHT potential had an incorrect cohesive energy for the crystal structures but did fit the experimental phase transition from the diamond structure to the β-tin structure quite well. Several other potential functions have also been advanced by Tersoff,[20–22] Biswas and Hamann,[23,24] Dodson,[25] and Brenner and Garrison.[26] (The three Tersoff potentials in Refs. 20, 21, and 22 will be referred to as TER1, TER2, and TER3, respectively; the two potentials of Biswas and Hamann in Refs. 23 and 24 will be denoted BH1 and BH2, respectively.) Most recently a series of model potentials, termed classical force fields (CFF), have been proposed by Chelikowsky, Phillips, Kamal, and Strauss (CPKM) (Refs. 10 and 27) and by Wang and Messmer.[28] In some cases these agree with the *ab initio* geometries for the clusters but do not reproduce the energetics very well. The CPKM thermodynamic interatomic force field (TIFF) seems the most promising of these and has recently been applied to silicon clusters.[29] It has not been tested for surface properties or crystal defects. Khor and Das Sarma[30,31] have developed a flexible analytic potential for silicon that seems promising, unfortunately it uses a slightly different functional form and parameter set for modeling the surface and bulk crystal behavior. Another potential has recently been proposed by Baskes[32] that is based upon a modification of the embedded-atom method.[33,34] This has proven extremely powerful in modeling fcc metals but how well it represents covalent systems has yet to be determined. In many ways the present work has been inspired by all of

these earlier attempts and builds upon and uses those ideas that are deemed most useful from each of these methods.

There are several reasons why it has proven so difficult to develop a totally satisfactory potential for silicon. Clusters of four or more atoms typically have a multitude of configurations that are local minima on the potential-energy surface. These involve silicon atoms with high coordination numbers and strained bond angles. The penalties caused when an atom forms a strained bond angle are offset by the large number of weak bonds formed. This suggests that there is no large energy penalty associated with distortion of the bond angles away from 109°. This is in contrast to the diamond lattice, where the resistance to distortions of the bond angles is quite large. A valid potential must therefore incorporate angle dependences that are different for the clusters and the crystal. In addition, one must deal with the problem of multiple bonding in the small clusters. If one compares the cohesive energy per bond (E_b) in the small clusters and the crystal one finds E_b(linear trimer) $> E_b$(dimer) $> E_b$(crystal). This, together with information on the equilibrium bond lengths in the dimer and crystal, suggests that the dimer and trimer are stabilized by π bonding that is not present in the crystal. Ragavachari and Rohlfing have shown that for silicon clusters, with 2–10 atoms, a variety of hybridizations of the silicon atoms is present.[5] Wide variations can even occur in a single cluster. The overall problem of determining a potential for both silicon bulk and clusters has been summed up by Tersoff[21] as the "polymorphous perversity" of silicon.

In this paper we present a potential that is a generalization of the "Tersoff form," in which the environment dependence in the bond energy is incorporated into an interference function included in the two-body potential. In our potential, the two-body interaction is expressed as a sum of π- and σ-bonding terms, each of which is independently influenced by the environment. This is a flexible approach for developing a potential function that can fit a wide range of data. The parameters in the potential have been chosen to fit data on both small clusters and bulk materials. We will present results on the structure and energetics of clusters, bulk crystals, and surfaces of silicon. The potential will be used, in the future, in molecular-dynamics calculations to study cluster dynamics and equilibrium structures, the bulk crystalline, amorphous, and liquid phases, as well as the structure and dynamics of surface phenomena such as adsorption and diffusion.

In order to clarify later discussions of the form of the potential we used, and of our fitting procedure, we list the main pieces of information that we have used in developing the functional form of the potential and obtaining the parameters in the potential.

(1) We have used the available data on equilibrium cluster geometries and cohesive energies, given by *ab initio* calculations, for clusters of 2–10 silicon atoms. This includes data on the global energy minimum for each cluster and other local minima as well. Much of the quantum data we used was from the series of articles by Ragavachari, Rohlfing, and Logovinsky.[1–5,35] All *ab initio* energies taken from the literature were based on the restricted Hartree-Fock (RHF) calculations with correlation energy included by using Møller-Plesset perturbation theory to fourth order (MP4). This method is size consistent. Size consistency is important if we are to compare energies of various sized clusters. The 6-31 G* basis set was used throughout. Ragavachari noted that 80–85 % of the experimental binding energy of Si_2 and Si_3 is obtained at this level of theory. We followed his procedure of multiplying all *ab initio* cohesive energies by 1.2 to obtain a reasonable estimate of the correct values for the larger clusters. We also performed *ab initio* calculations at the unrestricted Hartree-Fock (UHF) and RHF levels of theory using the 6-31 G* basis set and MP4 perturbation theory for Si_2, Si_3, and Si_4 clusters to increase the variety of configurations in our potential-energy data base. (When we needed potential-energy curves for a range of nuclear positions, rather than energies at a small number of specific configurations, we preferred to use UHF/MP4 calculations. Potential-energy curves obtained by this method behave correctly in the limit as a cluster is dissociated into one or more open-shell fragments.)

(2) The static properties of the diamond crystal phase of silicon, including the cohesive energy, elastic constants, and lattice parameters were used.

(3) We have used the experimental facts that the diamond crystal structure is the most stable phase at low temperatures and pressures and that at low temperatures, as the pressure is increased, the first phase transition to occur is to a β-tin phase. A potential function was considered acceptable only if it was consistent with these facts.

(4) The point defect energies of the diamond-lattice interstitials and vacancies were required to be positive relative to the perfect diamond-lattice energy. This is a special case of the previous requirement that the diamond crystal structure be the most stable phase at low temperatures.

(5) The proposed model for the Si(111) 2×1 reconstruction that best agrees with experiment is that proposed by Pandey.[36] The Pandey structure suggests that π bonding is important in the 2×1 reconstruction. The functional form was adjusted to allow π bonding to stablilze this proposed Si(111) 2×1 π-bond-chain reconstruction.

We hope that by fitting the potential to data on small clusters we will be including much of the physics that is important for surface structure and energetics. At least our potential will have the ability to model undercoordinated and overcoordinated silicon atoms with distorted bond angles. We believe this will be instrumental in modeling surfaces and defects.

In Sec. II we will describe the actual functional form of the potential and the fitting procedure. The reasons for including the various terms will be explained. We will discuss the separation we have made into π- and σ-bonding terms. Section III will contain the results of our model for the clusters, crystals, and surfaces, as well as extensive comparisons with other potentials used to model silicon. Section IV will present the future directions

we wish to take in further testing and applying this potential to both surfaces and clusters.

II. POTENTIAL-ENERGY FUNCTION FOR SILICON

A. General Tersoff form

Tersoff[20,21] assumed that the total potential energy of interaction among a collection of N atoms could be written as a sum of environment dependent pair potentials:

$$V=\sum_{1\le i<j\le N} V_{ij} \ . \tag{1}$$

The interatomic potential between two atoms was taken to be of the form

$$V_{ij}=f_C(r_{ij})[V_R(r_{ij})+I_{ij}V_A(r_{ij})] \ . \tag{2}$$

Here V_R and V_A represent the repulsive and attractive parts of the potential energy, and f_C is a cutoff function for the interaction. The effect of the environment on the (i,j) bond is included in the I_{ij} factor. This inclusion of the bonding environment directly into the two-body interaction was proposed by Abell[37] and seems to be a promising direction for providing flexible and reasonable potentials for covalent systems. If one assumes this general form and places all many-body influences in I_{ij}, then the most difficult part of the problem involves finding an appropriate form for this interference.

For V_A and V_R Tersoff used the two exponential terms in a Morse potential. The coefficients in these terms are among the parameters that were chosen to fit his overall data base. Tersoff noted, from density functional theory results, that the energy per bond decreases monotonically with increasing coordination along the progression dimer→graphite→diamond→simple cubic. The energy per atom has a minimum for the diamond lattice, which has fourfold coordination. The desire to reproduce these trends led him to the two possible functional forms shown below:

$$I_{ij}=\frac{\exp(-\zeta_{ij}/a)+\exp(-\zeta_{ji}/a)}{2} \tag{3}$$

and

$$I_{ij}=\frac{(1+a^n\zeta_{ij}^n)^{-1/2n}+(1+a^n\zeta_{ji}^n)^{-1/2n}}{2} \ . \tag{4}$$

Here ζ_{ij} is a function of the environment of atom i, and ζ_{ji} is a function of the environment of atom j. The I_{ij} function is thus a function of the environment of the ij bond. The parameters in his TER2 potential were chosen to fit the experimental cohesive energy and bulk modulus of the diamond lattice and the theoretical relative energies of some of the other crystal phases. Tersoff pointed out that the set of parameters he obtained is probably not optimal for silicon, given the limited search of parameter space he made. He has since revised the parameters, while still using the functional form in Eq. (4), in order to improve the diamond-lattice elastic properties. Unfortunately, the resulting TER3 potential does not provide a good description of surface properties and clusters. We shall be making most of our comparisons with the TER2 potential, since it is more applicable to the global behavior of silicon. We have included some comparisons with the TER3 potential for properties for which TER3 obtains good results.

The Tersoff form is appealing because of the generality of the approach and the physical justification for the chosen form. In the results section of this paper we will present a comparison of Tersoff's potential and our potential, but it is worthwhile to mention some of the shortcomings that motivated the present model.

The TER2 potential was fit to the experimental cohesive energy, bulk modulus, and density of the diamond crystal phase of silicon. However, the elastic constants are not well modeled, especially the c_{44} term, which is an order of magnitude too small. The predicted interstitial and vacancy energies are close to theoretical estimates. This potential fails to predict the experimentally observed transition to the high-pressure β-tin crystal phase. This phase transition has proven difficult to represent for most of the other models in the literature as well. We have investigated the structures and energies of small clusters and found that the TER2 potential gives structures for large clusters that are in good agreement with *ab initio* estimates, but it fails for small clusters where π bonding is important. As we will discuss in the results section, it seems that the overall structure of the Tersoff potential-energy surface, for large clusters, is similar to the *ab initio* surface, at least with regard to the position of the minima on the surface. The major problem for large clusters is that his potential predicts cohesive energies that are too large.

The poor values for the elastic constants for TER2 are due to the softness of the bond-angle-bending contribution to ζ_{ij}. If the angle-bending contribution were made larger to correct this, it would drastically change the energies of the surfaces. It would change the predicted minimum-energy geometries and overall potential-energy surface to one similar to the SW surface, which, as we will show, is qualitatively different from the *ab initio* potential surface. We have confirmed this by testing Tersoff's TER3 (Ref. 22) potential on clusters. Even though TER3 managed to correct the elastic constants, we find the clusters to be much less well modeled. Some of the problems in Tersoff's potential are due to the less than optimal choice of parameters; yet it is unclear that even an optimal set could provide good results for all of the diverse bonding situations, especially small clusters with extensive π bonding.

Tersoff has attempted to obtain a potential for many diverse types of bonding by fitting to the dimer, graphite, diamond, and then the higher-coordination hypothetical phases. We believe that the drastic interpolation between the dimer and the solid phases is one of the shortcomings of his potential. We believe that our model will provide a more accurate interpolation, since it has been fit to more diverse bonding situations, including the bonding in clusters of silicon atoms.

B. A new potential for silicon

In an attempt to model silicon in all of its diverse bonding situations, we approached the problem with a

simple generalizable function. As already stated, Tersoff's form of an environment-dependent two-body interaction was our starting point. We assumed a simple functional form for the potential. The parameters were chosen to fit data on the clusters and on the bulk phases. We then introduced changes in the functional form only when it was clear that there was some bonding situation for which the potential was deficient.

For each functional form chosen, we first adjusted the parameters to fit the *ab initio* cluster energies for Si_2–Si_{10}. After fitting the clusters we used the potential to calculate the properties of the diamond crystal structure, the values of the interstitial and vacancy energies, and the relative energies of other crystal phases. If the potential gave poor results we would modify the parameters to obtain, if possible, better results for the bulk properties. The new parameters would be tested by applying the potential to clusters once again. If the potential was judged to be inadequate we would modify the potential to increase its complexity and flexibility. The new functional form was then subjected to the same procedure of adjustment of parameters and testing. By this iterative process, the potential function became more flexible and more complicated.

At each stage of this iterative development of the potential, the type of complication that was introduced was determined by what we felt to be the major deficiency of the preceeding form. This involved subjective decisions of what was important and nonunique choices of how to make the potential more flexible. Thus the resulting functional form is in no sense unique. Many aspects of it have no simple physical interpretation; the basic justification is that we found it necessary to have something this complicated to achieve the quality of fit that was desired. It is entirely possible that some totally different form might be more simple as well as more accurate. One feature of the resulting potential does have a simple physical interpretation. We found it useful to separate the attractive portion of the potential into π and σ bonding terms, each of these being independent functions of the environment.

The final potential-energy function we obtained is

$$V=\sum_{1\le i<j\le N} V_{ij} \ , \tag{5}$$

$$V_{ij}=f_C(r_{ij})[V_R(r_{ij})+I_{ij}^{\pi}V_{\pi}(r_{ij})+I_{ij}^{\sigma}V_{\sigma}(r_{ij})] \ , \tag{6}$$

where the I_{ij} functions are termed the "interference" functions. In order to help us define the separation of V_A into V_σ and V_π, we imposed restrictions on the form of the interference functions. First we demanded that $I_{ij}^{\pi}=I_{ij}^{\sigma}=1$ for Si_2 (no neighbors are present to interfere with the bonding). We expected π bonding to be unimportant in the diamond lattice. Hence I_{ij}^{π} was constructed such that $I_{ij}^{\pi}=0$ for the diamond crystalline solid and for small distortions of that structure. We demanded that $I_{ij}^{\sigma}=1$ for the diamond lattice and small uniform compressions and dilations of the structure, but not for other distortions such as shearing. These conditions were sufficient to allow us to define the various terms in the potential-energy function.

For V_A and V_R in Eq. (2), Tersoff used the two exponential terms obtained from a Morse potential fit to his overall data base. We prefer to define the separate attractive and repulsive curves on the basis of quantum-mechanical calculations of various dimer potential-energy curves, in the following admittedly heuristic way.

We imagine that the repulsive function V_R represents Pauli exclusion of overlapping occupied orbitals on the two atoms of a dimer. The attractive function is made up of V_σ and V_π contributions that represent covalent bonding due to the favorable interaction derived from putting electrons into bonding σ and π orbitals. We expect that a reasonable representation of these three functions would give $V_R(r)$ as a positive, monotonically decreasing, short-ranged function of r and $V_\sigma(r)$ and $V_\pi(r)$ as negative, monotonically increasing, longer-ranged functions of r. All three contribute to the ground-state dimer potential-energy surface. Thus, applying (5) and (6) to a pair of Si atoms, we obtain

$$V^{\text{bond}}(r)=V_R(r)+V_\pi(r)+V_\sigma(r) \ , \tag{7}$$

where $V^{\text{bond}}(r)$ is the ground-state potential-energy function of a silicon dimer (which is a triplet state). We have used the assumption, noted above, that the interference functions are unity for an isolated dimer.

Imagine a silicon dimer with the two nuclei lying along the z axis. The covalent σ bonding in the ground state arises from putting two electrons with opposite spin in a bonding σ orbital made primarily from the valence p_z orbitals on each Si, which lie along the internuclear axis. The π bonding arises from having one unpaired electron in each of two π orbitals. One of the π orbitals is primarily made of the valence p_x orbitals on each atom, and the other is primarily made of the valence p_y orbitals on each atom. There is an excited state of the silicon dimer, for which quantum calculations can be performed, in which this σ and π bonding are frustrated in the following way. Two electrons with the same spin are forced to be in (necessarily different) p-σ orbitals made up of atomic p_z orbitals, and two electrons with the same spin are foced to be in (necessarily different) p-π orbitals made up of atomic p_x orbitals. For this state, the interactions among the various valence electrons lead to interactions that are analogous to those in the ground state of the dimer but that are repulsive rather than attractive. With this as motivation, we assume that

$$V^{\text{anti}}(r)=V_R(r)-V_\sigma(r)-V_\pi(r) \ , \tag{8}$$

where $V^{\text{anti}}(r)$ is the potential-energy curve for the excited state described above. We now combine Eqs. (7) and (8) to obtain

$$V_\sigma(r)+V_\pi(r)=\frac{V^{\text{bond}}(r)-V^{\text{anti}}(r)}{2} \tag{9}$$

and

$$V_R(r)=\frac{V^{\text{bond}}(r)+V^{\text{anti}}(r)}{2} \ . \tag{10}$$

Equation (10) is an explicit equation for the repulsive potential in terms of two well-defined potential-energy

curves for a silicon dimer. Equation (9) gives the sum of the σ and π potentials. The σ and π functions can be obtained separately by considering the diamond crystal structure and its isotropic expansions and contractions. For such structures, we have demanded that $I^{\sigma}=1$ and $I^{\pi}=0$. Thus the energy of such a crystal is

$$E=2N[V_R(r)+V_{\sigma}(r)] , \tag{11}$$

where r is the near-neighbor distance and N is the number of atoms in the crystal. This follows from Eqs. (5) and (6) and applies for values of r for which interactions between only nearest neighbors contribute to the energy. [The cutoff function f_C in Eq. (6) will be chosen so that this range of r includes the equilibrium distance in the crystal.] We arbitrarily chose V_{π} to be an attractive function with three parameters:

$$V_{\pi}(r)=a_1\{\tanh[a_2(r-a_3)]-1\} . \tag{12}$$

This gives

$$V_{\sigma}=\frac{V^{\text{bond}}(r)-V^{\text{anti}}(r)}{2}-a_1\{\tanh[a_2(r-a_3)]-1\} . \tag{13}$$

We choose the three parameters in V_{π} so that, when Eq. (13) is substituted into Eq. (11), the result is consistent with the cohesive energy, bulk modulus, and bond length of crystalline silicon. With the three chosen parameters V_{π} is short ranged (vanishing almost completely at 2.9 Å, see Fig. 1).

$V^{\text{bond}}(r)$ and $V^{\text{anti}}(r)$ were obtained by performing UHF/MP4/6-31G* calculations on the ground state and the excited state mentioned above. The numerical values were rescaled by a factor of 1.2 (see discussion above) and fit to the following functional forms, often referred to as the extended Rydberg potential:

$$V^{\text{bond}}(r)=-D_e\left[1+\sum_{i=1}^{6} b_i\rho^i\right]\exp(-b_1\rho) \tag{14}$$

and

$$V^{\text{anti}}(r)=(b_8+b_9\rho+b_{10}\rho^2)\exp(-b_7\rho) . \tag{15}$$

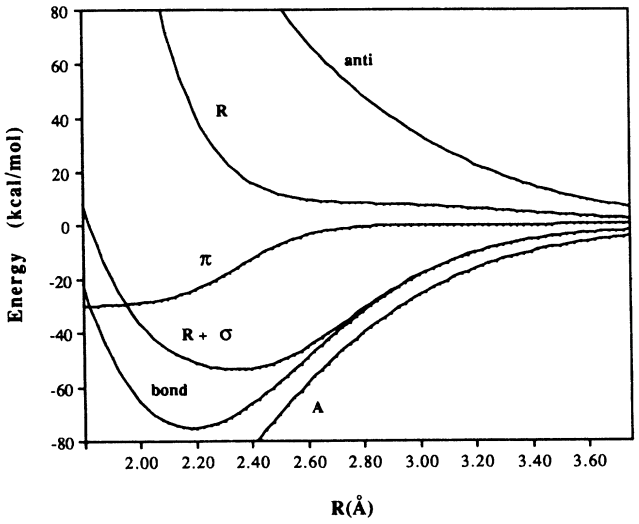

FIG. 1. The two-body potential-energy functions defined in our potential. The label of these curves are from the subscripts of the appropriate potentials defined in the text. The *bond* and *anti* curves are the quantum surfaces described by Eqs. (14) and (15). The R and A curves are from Eqs. (9) and (10), respectively. The π curve is the π-bonding part of the attractive interaction defined in Eq. (12). Note that *bond* is the potential energy felt by the isolated dimer, and $R+\sigma$ is the potential when no π bonding is present (i.e., in the diamond lattice phase of silicon).

In both of the above equations $\rho=r-r_e$, and r_e is the equilibrium distance for the ground-state energy surface of the dimer (2.184 Å). The values of the parameters in V^{bond}, V^{anti}, and V_{π} are given in Table I and the functions are shown in Fig. 1.

The cutoff function $f_C(r)$ in Eqs. (2) and (6) is taken to have the same form as Tersoff's cutoff function:

$$f_C(r)=\begin{cases} 1, & r<R-D \quad (16a)\\ \frac{1}{2}-\frac{1}{2}\sin[\frac{1}{2}\pi(r-R)/D] , & \\ \qquad R-D<r<R+D & (16b)\\ 0, \quad r>R+D , & (16c)\end{cases}$$

TABLE I. The coefficients for the various functions defined in the present potential. The b coefficients were fit to the two-body interaction surfaces and the c parameters for the π switching function were chosen arbitrarily. The a and d coefficients were chosen to fit the data on clusters and crystals.

$a_1=15.211$ (kcal/mol)	$b_1=2.8350$ Å^{-1}	$d_0=0.005\,387$
$a_2=4.0900$ Å^{-1}	$b_2=0.7296$ Å^{-2}	$d_1=0.007\,894$
$a_3=2.3650$ Å	$b_3=-2.2965$ Å^{-3}	$d_2=-0.081\,615$
$a_4=0.0090$	$b_4=-1.3677$ Å^{-4}	$d_3=-0.083\,367$
$a_5=0.0100$	$b_5=2.0485$ Å^{-5}	$d_4=0.380\,043$
$a_6=1.0000$	$b_6=-0.4745$ Å^{-6}	$d_5=0.374\,569$
$a_7=0.3333$	$r_e=2.184$ Å	$d_6=0.054\,232$
$a_8=0.4521$	$D_e=75.47$ kcal/mol	$c_1=-175.0$
$a_9=-0.8763$	$b_7=3.4835$ Å^{-1}	$c_2=240.0$
$a_{10}=1.8387$	$b_8=165.16$ (kcal/mol)	$c_3=-108.0$
$a_{11}=75.3470$	$b_9=96.70$ (kcal/mol) Å^{-1}	$c_4=16.0$
$a_{12}=0.3425$	$b_{10}=495.73$ (kcal/mol) Å^{-2}	
$a_{13}=5.0000$		

where $R=3.60$ Å and $D=0.15$ Å. This will cut off the potential just short of the second nearest neighbor in the diamond lattice.

C. The interference functions

The question arises of how to represent the environment-dependent terms in the potential, i.e., the interference functions I^{π} and I^{σ}. We decided to assume that the degree of interference of one bond with another should change on the same distance scale as does the attractive bond energy of a Si—Si single bond. It is convenient to define a quantity $s(r_{ij})$ for a pair of atoms a distance r_{ij} apart, that is a measure of the extent to which they are bonded. We shall call this the bonding function. The definition which we use is

$$s(r)=\begin{cases}1, & r<r_e \qquad (17a)\\ f_C(r)\dfrac{V_R(r)+V_\sigma(r)}{V_R(r_e)+V_\sigma(r_e)}, & r\geq r_e\ , \qquad (17b)\end{cases}$$

where $r_e=2.35$ Å is the distance for the minimum of the σ bond. Thus $s(r)$ changes monotonically and with continuous slope from 1 to 0 as r increases from 0 to ∞. For clarity of notation we will, from now on, refer to $s(r_{ij})$ as s_{ij}. f_C is again the cutoff function.

Tersoff chose in his TER1 potential to represent the interference function in terms of his w functions, which are analogous to our bonding functions s, and cosines of angles between various bonds. Similarly we have chosen to use the bonding functions and the cosine function. Various polynomials and powers of polynomials appear in the interference functions in ways that are more complicated than the formulas used by Tersoff. In particular, certain polynomial terms were chosen to stabilize or destabilize various bonding topologies such as triangles, tetrahedra, and squares.

1. The σ-bonding interference

The σ-bonding interference function is expressed in terms of two factors, one that involves angles between bonds and the other that involves a polynomial in the bonding function. The functional form which we have chosen is

$$I_{ij}^{\sigma}=\frac{1}{1+Z_{ij}^{a_6}\left[\displaystyle\sum_{\substack{1\le k\le N\\(i\neq k\neq j)}} a_4 s_{ik}s_{jk}+\sum_{\substack{1\le k<l\le N\\(i\neq k\neq j,\\ i\neq l\neq j)}} a_5 s_{ik}s_{il}s_{jk}s_{jl}s_{kl}\right]}\,\frac{1}{1+Z_{ij}^{a_7}\left[\displaystyle\sum_{\substack{1\le k\le N\\(i\neq k\neq j)}}[s_{ik}P(\theta_{jik})+s_{jk}P(\theta_{ijk})]\right]}\ , \qquad (18)$$

where

$$Z_{ij}=\sum_{\substack{1\le k\le N\\(i\neq k\neq j)}}(s_{ik}+s_{jk}) \qquad (19)$$

represents the coordination of the bond (i,j) of interest. In this notation θ_{ijk} is the angle at atom j of the triangle whose vertices are the positions of atoms i, j, and k.

In order to correctly model the elastic constants of the silicon diamond lattice the $P(\theta)$ term must have a minimum at the tetrahedral angle and a second derivative appropriate to the elastic constants. We initially chose $P(\theta)$ to be a quadratic function of $\cos(\theta)$, namely $a[\cos(\theta)+\frac{1}{3}]^2$. If a was chosen to give good elastic constants, then it was difficult to obtain a phase transition from the diamond to β-tin structures at high pressure, as well as good relative energies for the other crystal phases. This form for $P(\theta)$ also caused the cohesive energies of the clusters to be too low. We increased the flexibility of $P(\theta)$ by making it a sixth-order polynomial and varying the coefficients subject to the constraint that we still obtain good first and second derivatives at the tetrahedral angle of 109.47°:

$$P(\theta)=\sum_{n=0}^{6} d_n\cos^n(\theta)\ . \qquad (20)$$

The polynomial $P(\theta)$ has a second, slightly higher, minimum at 70°. This second minimum allows less weakening of the bond when it has neighbors at or near this smaller angle. This angle dependence of the σ interference function was needed to make the β-tin structure have a cohesive energy in accordance with experiment, but an interference function with only the $P(\theta)$ contribution would lead to calculated fcc and bcc energies that are lower than that of the diamond lattice. In addition the T (tetrahedral) and H (hexagonal) self-interstitials in the diamond crystal were found to be too stable. We then included the three-body and four-body polynomial terms, $a_4 s_{ik}s_{jk}$ and $a_5 s_{ik}s_{jk}s_{il}s_{jl}s_{kl}$, which destabilized the defects and the close-packed crystal phases. Once this was done the defects were modeled adequately and the cohesive energies of the close-packed crystals were less stable than diamond but were competing with β tin. A slight additional destabilization of the close-packed structures was produced by including the coordination number dependence, $Z_{ij}^{a_6}$ and $Z_{ij}^{a_7}$, as factors that affect the strength of the three-body, four-body, and $P(\theta)$ terms. This coordination dependence also decreases the effect of these terms on some small clusters, where compact structures are present.

2. π-bonding interference

We assume that π bonding occurs when a bond and its neighboring atoms (if any) are close to a planar configuration. The largest coordination that is typically

allowed for the atoms that form π bonds is 3. Thus π bonding occurs in graphite structures, or in small clusters that are planar or of low coordination. Quantum calculations have shown that π bonding is important in silicon clusters with 2–6 atoms. It is also important for some surface properties, especially Pandey's proposed 2×1 reconstruction of the Si(111) surface[36,39] and possibly the Si(100) 2×1 dimer reconstruction. We expect π bonding to be nonexistent in the diamond-lattice structure, which is a classic situation of pure σ bonding using hybridized orbitals. We have found that modeling π bonding for this wide range of situations is extremely difficult. We have had to construct an interference function that is more complex than was needed for the σ bonding.

A way to model π-bonding interferences is in terms of deviations from planarity. For any four atoms, we use the volume of the parallellepiped formed by the four atoms, divided by the bond lengths that determine the sides of the parallellepiped:

$$v_{ijkl}=\mathbf{r}_{ij}\cdot\mathbf{r}_{jl}\times\mathbf{r}_{ik} \ . \tag{21}$$

Since we desire a harmonic restoring force for small deviations from planarity, we use the square of this volume in the potential function. Several other polynomial terms are also included to increase the flexibility of the potential in describing the small clusters. The final form of the π-bonding interference function is

$$I_{ij}^{\pi}=S(Z_i^j)S(Z_j^i)\exp\left[-\sum_{\substack{1\le k\le N\\(i\neq k\neq j)}}F_3-\sum_{\substack{1\le k<l\le N\\(i\neq k\neq j,\\ i\neq l\neq j)}}F_4-\sum_{\substack{1\le k<l<m\le N\\(i\neq k\neq j,\\ i\neq l\neq j,\\ i\neq m\neq j)}}F_5\right] . \tag{22}$$

Here $S(Z_i^j)$ is a switching function of the form

$$S(Z)=\begin{cases}1, & Z\le 2 & \text{(23a)}\\ c_1+c_2Z+c_3Z^2+c_4Z^3, & 2\le Z\le 2.5 & \text{(23b)}\\ 0, & 2.5\le Z\ , & \text{(23c)}\end{cases}$$

and Z_i^j is the coordination of atom i, excluding atom j,

$$Z_i^j=\sum_{\substack{1\le k\le N\\(i\neq k\neq j)}}s_{ik} \ . \tag{24}$$

This will turn off the I_{ij}^{π} term as the number of additional bonds around either atom i or j goes from 2.0 to 2.5. This will effectively turn off π bonding in the compact clusters with more than six atoms and in the bulk crystal phases. The π bonding must be completely turned off in the diamond lattice in order for the separation of V_σ and V_π to be performed in the manner discussed above. The F_3, F_4, and F_5 functions are the three-body, four-body, and five-body polynomial terms needed to fit the π bonding in small clusters:

$$F_3=a_8s_{ik}s_{jk}+\frac{a_9[s_{ik}(1-s_{jk}^4)+s_{jk}(1-s_{ik}^4)]}{1+Z_{ij}} \ , \tag{25}$$

$$F_4=a_{10}(s_{ik}s_{il}s_{jk}s_{jl})+\frac{a_{11}[s_{ik}s_{jl}(1-s_{il})(1-s_{jk})+s_{il}s_{jk}(1-s_{ik})(1-s_{jl})]}{1+Z_{ij}^5}$$
$$+a_{12}\frac{v_{ijkl}^2}{|r_{ij}|^2}\left[\frac{s_{ik}s_{jl}}{|r_{ik}|^2|r_{jl}|^2}+\frac{s_{il}s_{jk}}{|r_{il}|^2|r_{jk}|^2}+\frac{s_{ik}s_{il}}{|r_{ik}|^2|r_{il}|^2}+\frac{s_{jk}s_{jl}}{|r_{jk}|^2|r_{jl}|^2}\right] , \tag{26}$$

$$F_5=a_{13}(s_{ik}s_{jk}s_{il}s_{jm}s_{kl}s_{km}+s_{ik}s_{jk}s_{im}s_{jl}s_{kl}s_{km}+s_{il}s_{jl}s_{ik}s_{jm}s_{kl}s_{lm}$$
$$+s_{il}s_{jl}s_{im}s_{jk}s_{kl}s_{lm}+s_{im}s_{jm}s_{ik}s_{jl}s_{km}s_{lm}+s_{im}s_{jm}s_{il}s_{jk}s_{km}s_{lm}) \ . \tag{27}$$

The $a_8s_{ik}s_{jk}$ term is a three-body term that represents the interference with π bonding between atoms i and j when both atoms are bonded to a common neighbor k. The a_9 term is present only to stabilize the linear trimer. The a_{10} term is similar to the a_8 except that it represents interference in π bonding when atoms i and j are both bonded to two common nearest neighbors. The a_{11} term is used to destabilize ring structures. Its effect decreases rapdily with coordination so that it only acts upon open rings and not on other planar structures. The a_{12} term includes the volume function described above in Eq. (21) and allows I^{π} to favor planar structures. Finally, F_5 is a five-body term that is needed to destabilize certain planar nonring structures. Its six terms involve simple permutations of k,l,m.

The most fundamental test of the usefulness of these terms is simply fitting the clusters with and without each term to find the set that is necessary in order to obtain the best overall fit and correct minimum-energy geometries for the clusters. In fact, many other polynomial terms, not mentioned here, have been tried and have proven less effective in modeling Si clusters. Of course, the full justification of this potential can only be understood in light of the attempt to obtain a global fit to many different bonding situations. It is also important to remember that this model can be greatly simplified if one wants to fit only certain situations. The a_9, a_{11}, and a_{13} terms could be eliminated if one were not interested in representing the small clusters. The a_8, a_{10}, and a_{12} terms would still be able to represent surface π bonding.

D. Summary

The potential we are proposing for silicon is completely defined by Eqs. (5), (6), (10), and (12)–(27), together with the parameters in Table I. In the remainder of this paper, we shall present various results calculated with this potential and compare them with experimental data and with results calculated with other potentials that have been proposed for silicon.

III. RESULTS

A. Silicon clusters

We have attempted to find a potential that would give correct geometries and binding energies for the global potential energy for clusters of various sizes, have additional minima for geometries where quantum mechanics indicates there are low-energy local minima, and not have any low-energy local minima that are absent from the true quantum-mechanical surface. In addition, we wanted the potential-energy function to generate correct curves for the energy as a function of distance as an atom is removed from a cluster. In other words, we wanted the overall shape of the multidimensional potential-energy surface to be correct for low-energy configurations. We were less concerned about achieving an accurate fit to the true surface for very high-energy configurations, provided that the function also generated large values of the energy for such configurations. We believe that all of these criteria are important if molecular-dynamics calculations of clusters and condensed phases are to be performed. If experimental cluster fragmentation studies like those performed by Bloomfield, Freeman, and Brown[40] are to be understood in terms of atomic processes, then the various pathways to dissociation have to be described accurately. To model this type of fragmentation, a potential should represent, as well as possible, the total-potential-energy surface, and not just the global minima.

The quantum-mechanical results for clusters are summarized below and compared with our own and other potentials. The *ab initio* results are taken from Ragavachari and co-workers.[1–5] We refer to the cluster geometries with a notation that is, as much as possible, consistent with Ragavachari's. To find the energies and geometries of local and global potential-energy minima for all of the potentials, we have used both search and steepest-descent methods from a set of initial configurations. Several initial geometries were chosen for each cluster, including the geometries corresponding to the various minima on the quantum potential-energy surface. We have also used the results already obtained for the minimum energy geometries of the SW potential.[17,18]

The present model was compared to Tersoff's second potential[21] (TER2), the potential of Stillinger and Weber[14] (SW), and the second potential of Biswas and Hamann[24] (BH2). Figure 2 shows the (binding energy)/atom as a function of cluster size. We obtain good fitting to the energetics of the clusters. Only for Si_7 is there a serious discrepancy. For clusters with 5–7 atoms, the transition is occurring in which π bonding be-

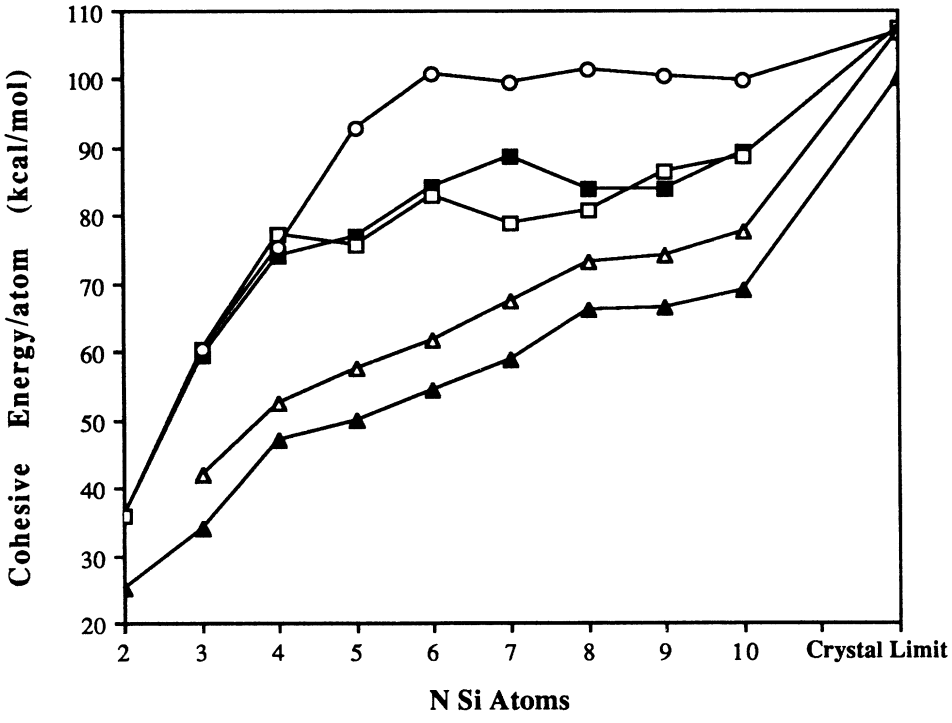

FIG. 2. Cohesive energy per atom for small clusters of silicon atoms at their global minimum potential energy and for the bulk crystal. The symbols denote "correct" (■), present (□), TER2 (○), BH2 (△), SW (▲). The "correct" numbers for clusters are the results obtained from *ab initio* RHF or UHF quantum-mechanical calculations at the UHF/MP4/6-31G* level, multiplied by 1.2. See the discussion in the text. They represent the best estimate for the correct energies of clusters. The "correct" number for the crystal is from experiment (Ref. 15).

comes less important, and more compact structures become energetically favored. This is difficult to model correctly and could be part of the problem with our calculated cohesive energy of Si_7. Tersoff's potential has the correct overall shape of this curve, but it predicts cohesive energies that are too large and approach the crystal limit much too quickly. Both the Stillinger-Weber and Biswas-Hamann potential predict cohesive energies that are too small.

If a potential-energy function were optimal, there would be a one-to-one correspondence between the local minima on its surface and the local minima on the true quantum-mechanical surface. Moreover, the relative and absolute energies and the geometries of the corresponding minima should be in close agreement, especially for the lowest minima. None of the potential-energy functions, including our own, satisfied all these conditions for all the clusters. Various types of discrepancies were observed. The least important are small quantitative differences between the minima. The most serious are the absence of minima on the function surface that are present on the true surface, or vice versa. Of intermediate, but less serious, concern is the situation in which a minimum on one surface with symmetric structure corresponds to a set of symmetry-related minima on another surface. In Table II we show the binding energies of the local minima on the quantum-mechanical surface and on the surface of the various potentials. The corresponding structures are shown in Figs. 3–9.

For Si_4, Si_7, and Si_9 we obtain global minima that are of the same symmetry as the predicted quantum-mechanical global minima. For Si_3, Si_5, Si_8, and Si_{10} we obtain a local minimum that is of the same symmetry as the quantum global minimum. In addition, for Si_8 and Si_{10} our global minimum is in fact a local minimum on the quantum surface. For Si_6 Ragavachari obtains structure 6*a*, as his global minimum. We obtain 6*d* as our glo-

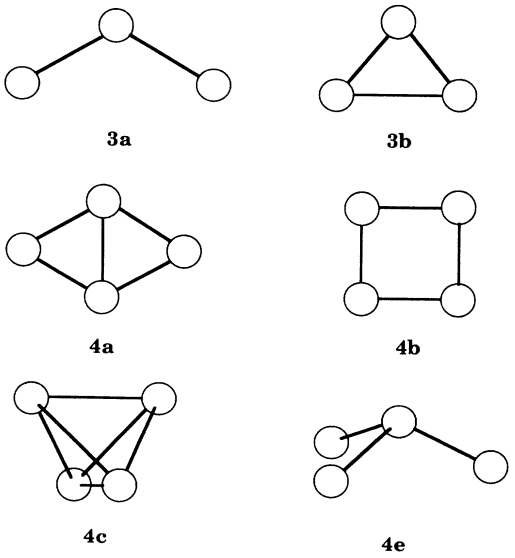

FIG. 3. Si_3 and Si_4 structures referred to in Table II. For Si_4 our potential has structure 4*a* as the global minimum, in agreement with quantum-mechanical results. The TER2 potential gives 4*c* as the minimum.

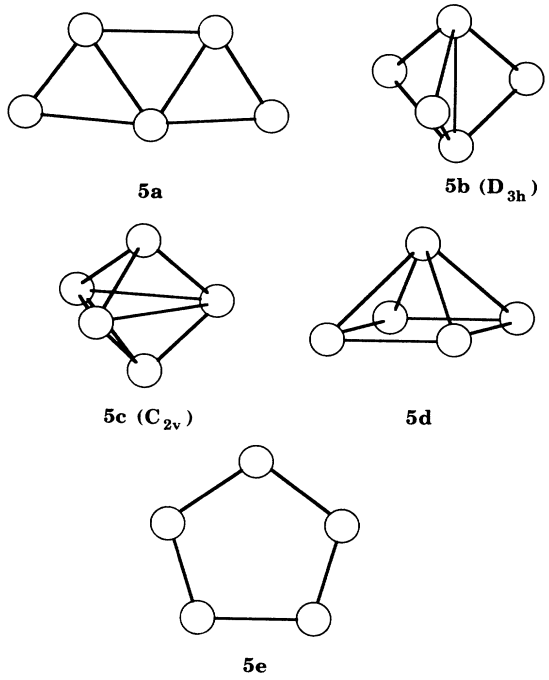

FIG. 4. Si_5 structures referred to in Table II. We find 5*a* as the global minimum and 5*c* and 5*d* as nearby local minima. The *ab initio* surface has 5*b* as the global minimum, and although 5*a* is close in energy, it is not a minimum.

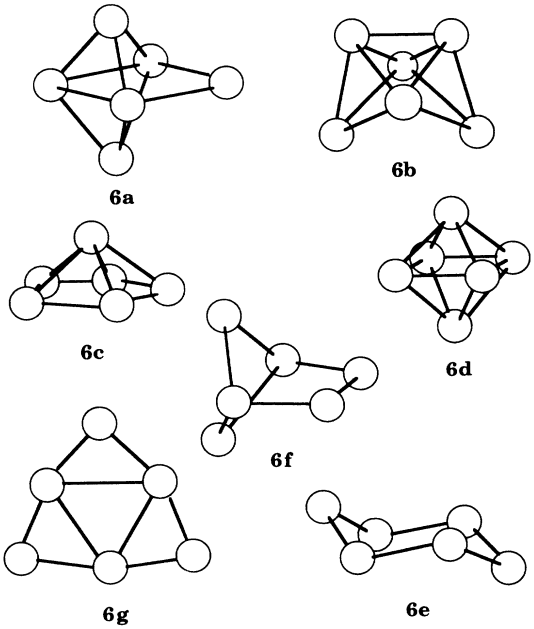

FIG. 5. Si_6 structures referred to in Table II. Our potential has some low-energy structures that involve π-bond stabilization (6*g*), but 6*d* is the global minimum. This is close to the Jahn-Teller distorted global minimum quantum structure 6*a*. Note that BH2 and SW favor the more open structures such as 6*f*. The fact that we obtain 6*g* as a low-energy structure indicates that our π interference function does not capture all the essential features of the π bonding. Tersoff's potential also gives 6*d* as the global minimum.

TABLE II. Binding energies (kcal/mol) of minima on the potential-energy surfaces. A ◇ represents a minimum for which we have no reported value of the energy. A * represents a structure that is not a minimum but for which the *ab initio* energy is known. The ? for structure 9*c* shows that there was some uncertainty as to whether this was a minimum on the quantum surface. In parentheses we have summarized the results for the different potentials. The format of this summary is discussed in the text. At the bottom of the table is a summary of the results for all clusters studied.

Structure	Quantum	Present	SW	TER2	BH2
2	75.5	75.5	50.0	60.5	57.3
		(1|1,1,0)	(1|1,1,0)	(1|1,1,0)	(1|1,1,0)
3*a*	177.6	178.0	99.9	120.9	
3*b*	178.0	186.2	102.3	181.4	125.48
		(2|2,0,0)	(2|2,0,0)	(2|2,0,0)	(2|1,0,0)
4*a*	296.3	300.1			
4*b*			187.5	241.9	210.2
4*c*	224.0	250.6	153.8	362.0	193.6
4*e*	◇	283.6	149.8	181.4	
		(3|3,0,0)	(3|2,0,1)	(3|2,0,1)	(3|1,0,1)
5*a*		361.0			
5*b*	385.2	316.4	247.2	391.4	280.4
5*c*	368.4	340.8			
5*d*		336.4	237.5	464.0	281.9
5*e*	232.3		249.6		287.6
		(3|2,0,2)	(3|2,0,1)	(3|1,0,1)	(3|2,0,1)
6*a*	505.2		322.6	532.0	364.7
6*b*	505*	438.2			
6*c*		443.6			
6*d*		452.1		604.3	
6*d*				362.8	352.7
6*e*	◇		326.0		369.5
6*g*		450.6			
		(2|0,2,1)	(2|2,0,0)	(2|1,1,1)	(2|2,0,1)
7*a*	621.3	549.8	374.4	695.6	459.3
7*b*	594.9	532.6		650.0	472.7
7*c*	563.9	547.3		686.0	
7*d*	519.4				
7*e*		507.6	412.6		
		(4|3,0,1)	(4|1,0,1)	(4|3,0,0)	(4|2,0.0)
8*a*				760.4	
8*b*	681.9	645.3			
8*c*	671.3			736.2	
8*d*	663.3	638.3			
8*e*	666.1	619.0		812.3	
8*g*		668.7			
8*h*			528.9		584.3
		(4|3,1,0)	(4|0,0,1)	(4|2,1,0)	(4|0,0,1)
9*a*	755	690.4		830.4	
9*c*	752?	790.8		903.6	
9*d*					667.9
9*e*			597.2		
		(2|2,0,0)	(2|0,0,1)	(2|2,0,0)	(2|0,0,1)
10*a*	893	742.9	534.3	901.1	673.1
10*c*	888	868.7		980.6	
10*d*	787	903.0		999.6	
10*e*			689.9		
10*g*			662.9		776.2
		(3|3,0.0)	(3|1,0,2)	(3|3,0,0)	(3|1,0,1)
		(24|19,3,2)	(24|11,0,7)	(24|17,2,3)	(24|10,0,6)

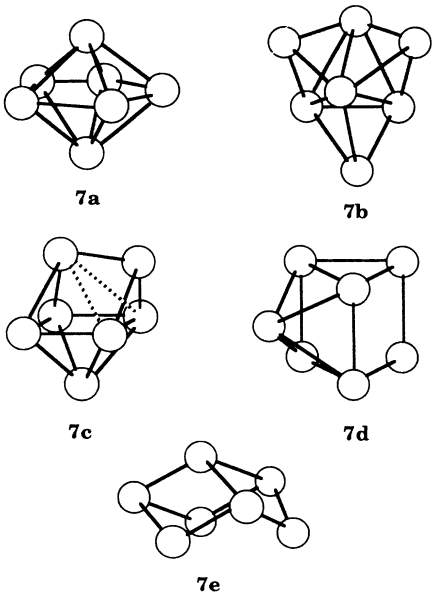

FIG. 6. Si_7 structures referred to in Table II. Both Tersoff's (TER2) and our potential agree with the quantum results in identifying 7*a* as the global minimum and 7*b* and 7*c* as low-energy local minima. For clusters this large, planar structures are not competitive with the compact structures in our potential.

bal minimum. Structure 6*a* can be thought of as a symmetry-broken 6*d*, where the top and bottom atoms of the octahedron have distorted to one side. The π interference function favors planar structures, and we obtain a low-energy, planar local minima for Si_6 that is incorrect. This demonstrates the difficulty in correctly

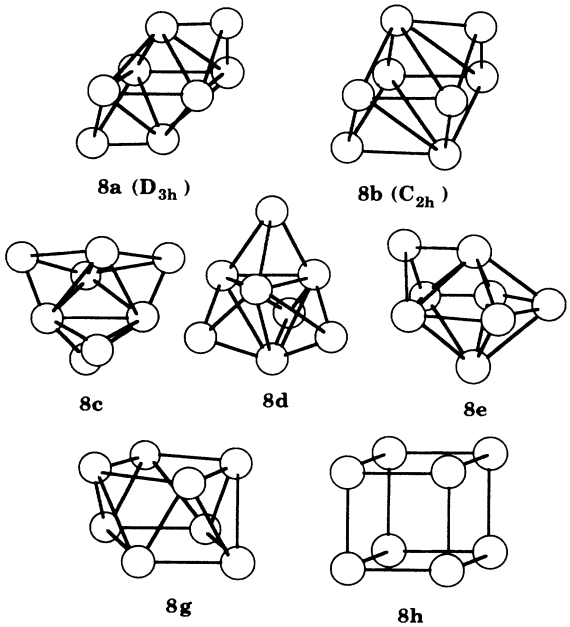

FIG. 7. Si_8 structures referred to in Table II. SW and BH2 both favor the cube (8*h*), while TER2 and our present model favor much more compact structures.

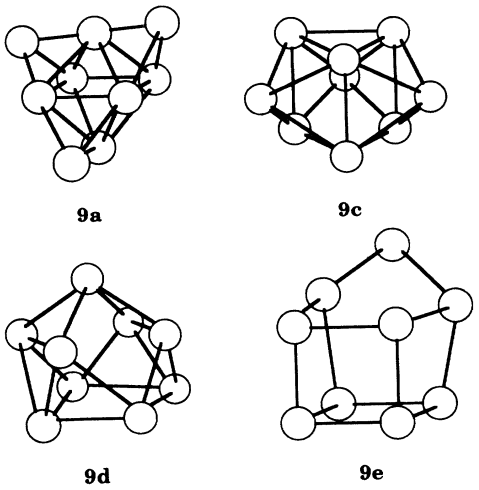

FIG. 8. Si_9 structures referred to in Table II.

representing some aspects of π bonding. Tersoff's potential does poorly for Si_4 and Si_5, where it gives a global minimum that is of the wrong symmetry and is much more stable than the other local minima. This is not surprising, since Tersoff did not attempt to model the π bonding in silicon. The SW and BH2 potentials have fewer local minima, and both have global minima, for most of the clusters, that are of the wrong symmetry. In fact, the SW and BH2 give very similar results for the clusters, which is due mainly to the fact that they have

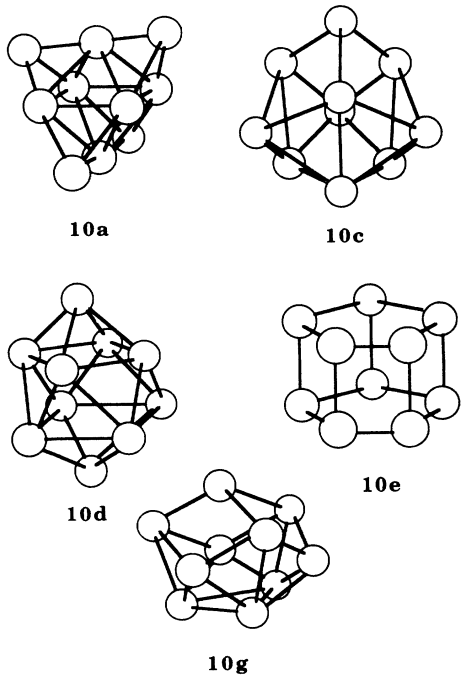

FIG. 9. Si_{10} structures referred to in Table II. It was found, for almost all models we tried, that the 10*d* structure was favored over 10*c*. This disagrees with the quantum results which find 10*d* to be about 80–100 kcal/mol higher in energy than 10*c* and 10*a*.

similar forms for their three-body potentials. It is seen that only Tersoff's and our potential give the wide variety of local minima that characterize the quantum surface. This is not too surprising, since both potentials are similar in form.

To provide a quantitative measure of the extent to which a potential-energy function has the correct number and types of local minima, we have devised a rating scheme of the following form: $(m|i,j,k)$. Here m is the total number of local minima that are known to exist on the *ab initio* surface, i is the number of minima on the surface of a potential function that are of similar geometry and the same symmetry as minimum on the *ab initio* surface, j is the number of minima on the surface of a potential-energy function that are of similar geometry to a minimum on the *ab initio* surface but that have a higher or lower symmetry than the *ab initio* minimum; and k is the number of minima found on the surface of the potential function that do not correspond to minima on the *ab initio* surface. (In counting minima, several minima that are related by symmetry are counted as a single minimum.) For a cluster with m minima, a perfect rating for a potential function would be $(m|m,0,0)$, i.e., all *ab initio* minima are present with the right geometry and symmetry, and no spurious minima are present. In Table II, this rating is given for each potential for each cluster size, and at the bottom the summary for each potential is given. For clusters from Si_2 to Si_{10}, the *ab initio* calculations have identified 24 minima. The present potential generates a surface that has 19 of them with the right symmetry and approximately the right geometry, and three with approximately the right geometry but incorrect symmetry. (Therefore, only two *ab initio* minima for these nine clusters are completely missing from the potential surface.) Meanwhile, only two spurious minima are present for the nine clusters. By this rating scheme, the TER2 potential is almost as good as the present potential in displaying the variety of minima seen on the *ab initio* surface, whereas the SW and BH2 potentials have fewer correct minima and more spurious minima.

When comparing all the various potentials, we see that the approach involving environment-dependent two-body potentials (Tersoff's and ours) seems to represent bonding in clusters in a more reasonable way. They also tend to give a different class of local minima from SW and BH2. Thus we have two qualitatively different types of multidimensional potential-energy surfaces. SW and BH2 would seem inadequate for MD studies of covalent clusters based upon these results. Tersoff's potential breaks down for small clusters, where π bonding is important. Tersoff's TER3 potential, in which the bulk behavior is improved, gives cluster results very similar to the SW and BH2 potentials.

In addition to the binding energy, the potential should describe dissociation correctly if it is to be used for dynamical studies of clusters. We show in Figs. 10–12 some representative dissociation curves for Si_3 and Si_4. This gives us some confidence that we are correctly modeling not only the minima but also the overall shape of the surface.

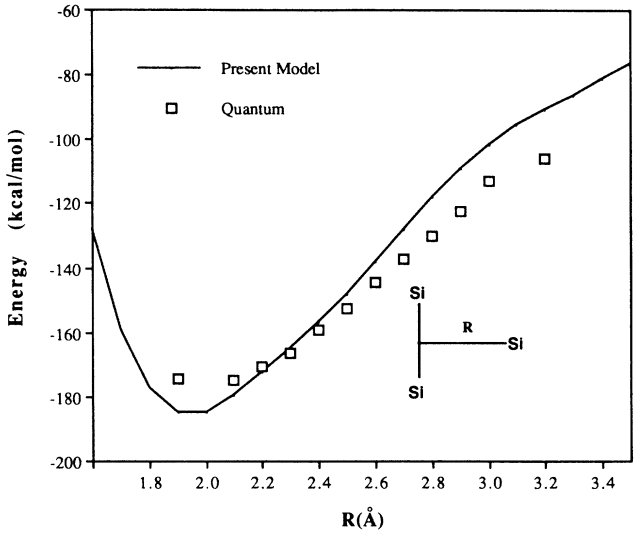

FIG. 10. The quantum- and potential-energy surfaces are compared for Si_3 when a silicon atom approaches a dimer along the perpendicular bisector. R is the length of the bisector. The quantum-mechanical results (UHF/MP4/6-31G*) are represented by (□).

B. Crystals

The most stable crystal structure for silicon, at all but very high pressures, is a diamond lattice. We have already stated that our potential has been chosen to give the experimental cohesive energy, bulk modulus, and density (lattice constant) for this phase. The elastic constants are very sensitive to the angular form of the σ interference function I_σ. The accuracy of the elastic constants (especially c_{44}) gives a good indication of how well the model is representing small angular distortion about

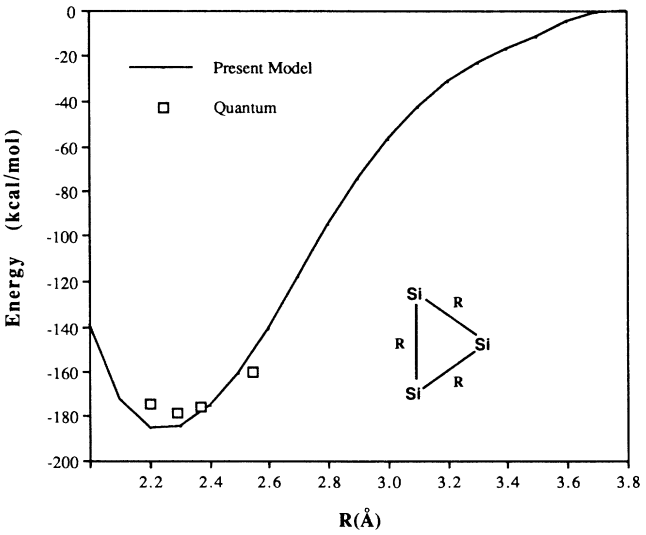

FIG. 11. The potential energy of the Si_3 equilateral triangle as a function of R, the Si-Si distance. The quantum results are at the UHF/MP4/6-31G* level.

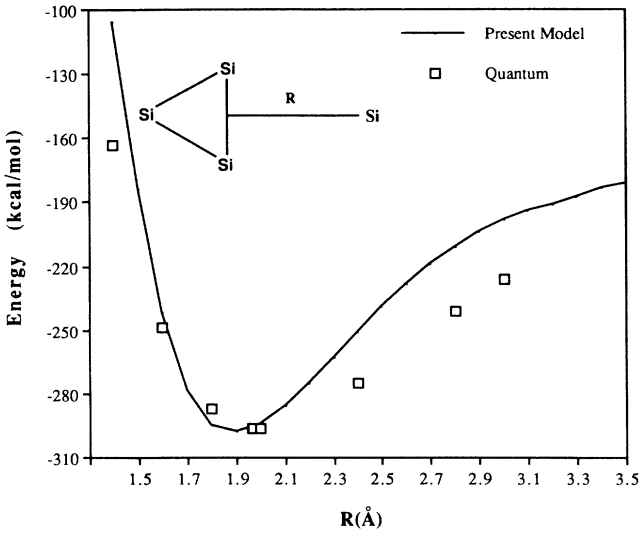

FIG. 12. The dissociation of Si_4 by removal of an Si from a planar rhombus structure. R is the distance from the center of the equilibrium structure to the silicon that is removed. The quantum results are at the UHF/MP4/6-31G* level.

the minimum. With the present choice of our potential parameters we obtain the results in Table III. The elastic constants are in excellent agreement with experiment. We also avoid the severe problem with shear displacements found for Tersoff's potential, caused by the weak angle dependence of his interference function and indicated by his low value for c_{44}. The Stillinger-Weber potential models the elastic constants reasonably but gives a cohesive energy of the crystal that is too low. In his third potential, Tersoff corrected the c_{44} elastic constant, but the range of the validity of this potential is limited to bulk behavior. For the phonon frequencies at the zone boundary we find results very similar to those found with the SW potential. The frequencies calculated using our potential are 10–15 % higher than experiment, except for a much larger error for the transverse acoustic (TA) mode. It should be noted that the present potential was not fitted to any phonon-dispersion data. The TER2 potential is in good agreement with experiment except for the frequency of the TA branch, which is too low. The TER3 potential produces very good agreement with most of the experimental frequencies, but gives a TA-branch frequency that is too high.

Next we consider the potential's ability to model defects in the diamond lattice. We have calculated the defect energy in a two-step procedure. We determined the energy of a large unit cell containing one defect, where the atoms in the cell had been relaxed. We then subtracted the energy of the same number of atoms in a perfect lattice. The point defects we have evaluated are the tetrahedral (T) and hexagonal (H) interstitials and the vacancy (V). We used a unit cell with 65 atoms for the interstitial and 63 atoms for the vacancy and allowed the atoms in the cell to relax. Tersoff used a unit cell with 217 atoms (215 for the vacancy). From tests we have performed on the convergence of the defect energy with increasing cell size (decreasing defect concentration) we believe that our results would not be greatly changed by using this larger cell. Our results are summarized in Table IV. There is no good experimental data on defect energies, although theoretical estimates based on the DFT-LDA suggest that the defect energies relative to the perfect crystal are in the 5–6-eV range for the T interstitial and 4–5 eV for the H defect.[41–44] All the calculated defect energies in Table IV are positive, as is necessary in order to be consistent with the experimental fact that the diamond lattice is the most stable crystal structure for silicon. The difference between our results for the T interstitial and the others is most likely due to the weak σ-bonding interference we incorporated for angles near 70° [see the discussion after Eq. (20)].

Finally, we have applied our potential to various other crystal phases, comparing the energy versus volume with experiment, the results of other models, and with the DFT-LDA results.[45–47] Real silicon is found to undergo a phase transition from the diamond to β-tin structure at high pressure (125 kbar at $T=77$ K). BH2 and TER2 predict a transition to a simple-cubic structure, while SW predicts no transition at all. Our potential gives a $T=0$

TABLE III. Properties of the diamond crystal phase of silicon. The cohesive energy, lattice constant, elastic constants, bulk modulus, and phonon frequencies at the zone boundaries are presented for the various potentials and compared with the experimental results. The phonon frequencies for the TER3 potential are from Ref. 22.

Parameter	Expt. (Ref. 38)	Present	SW	TER2	TER3 (Ref. 22)
Energy (kcal/mol atom)	106.7	107.3	100.1	106.7	106.7
a_0 (Å)	5.431	5.427	5.431	5.431	5.431
$c11$ (kcal/mol Å^3)	23.9	22.1	21.8	17.4	20.5
$c12$	9.20	10.1	11.0	12.4	10.9
$c44$	11.4	8.7	8.13	1.44	9.9
B_m (kcal/mol Å^3)	14.1	14.1	14.6	14.1	14.1
LTO(Γ) (THz)	15.5	17.9	17.8	16.7	16
TO(χ) (THz)	13.9	15.4	15.6	15.5	16
LOA(χ) (THz)	12.3	13.1	13.0	11.9	12
TA(χ) (THz)	4.5	7.0	6.5	2.8	9

TABLE IV. Point defect energies (eV) in the diamond crystal phase of silicon. T and H refer to tetrahedral and hexagonal interstitials, respectively.

	T interstitial	H interstitial	Vacancy
Present	0.8	3.0	4.5
TER2 (Ref. 21)	4.5	3.5	2.8
TER3 (Ref. 22)	3.8	4.7	3.7
BH2 (Ref. 24)	3.6	5.1	3.8
DFT (Refs 41–44)	5–6	4–5	3–4

K transition to a β-tin structure at approximately 250 kbar. The main reason for the discrepancy in the transition pressure is that the β-tin structure from our model is 10 kcal/mol higher in energy than diamond, whereas the experimental difference is about 6 kcal/mol. This, in conjunction with a density for β-tin that is about 12% too low in our model, gives the large discrepancy in the pressure. Of all the models that have been presented to this date, only the PTHT (Ref. 12) and our present potential are consistent with this phase transition. We have verified that, for our potential, the β-tin structure is mechanically stable at low temperatures and high enough pressures against small distortions in the shape and size of the unit cell.

Table V compares our present model with the DFT-LDA results for the various phases. We see that most of the crystal phases were predicted to be slightly too high in energy. (Note: $\Delta E_{\min} = E_{\min}^{\text{phase}} - E_{\min}^{\text{diamond}}$, where $E_{\min}^{\text{phase}}$ is the energy of a phase at the minimum of its E versus volume curve.) In a similar manner, all of the phases except the diamond crystal were predicted with the present model to have densities that are consistently about 10–15 % too low. It should be noted that only the β-tin phase is found experimentally, and these other theoretical phases should be considered less important in any fitting procedure. Figure 13 presents the energy versus atomic volume curves for these phases.

TABLE V. Relative energies of various crystal phases at their minimum in energy. DFT refers to the density functional theory results of Yin and Cohen (Refs. 45 and 46).

Crystal phase	$\Delta E_{\min}$ DFT (kcal/mol)	$\Delta E_{\min}$ Present
Diamond	0.0	0.0
β-tin	6.2	9.6
Simple cubic	8.1	9.2
HCP	12.7	16.1
Graphite	16.4	16.0
fcc	13.1	11.5
bcc	12.2	12.7

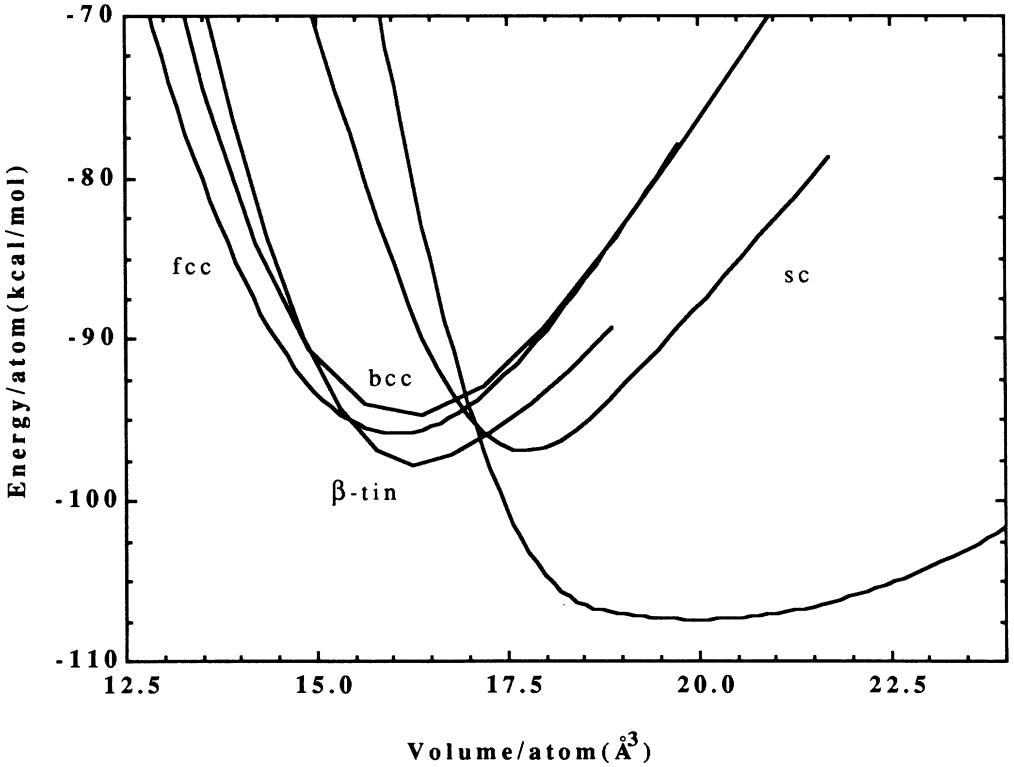

FIG. 13. Energy vs atomic volume for the various crystal phases calculated using our potential. Note that a common tangent construction implies the phase transition from diamond to β-tin at $T=0$ K.

C. Surface properties

The modeling of silicon surfaces is an important test for our potential. This tests the interpolative ability of the potential when dealing with both undercoordinated (relative to the bulk) and overcoordinated silicon. In addition, π bonding is thought to be important for some surface reconstructions, and it is important to test how well we are representing the π bonding for those situations. In deriving the functional form and parameters of our potential function, no surface data were used, except that the functional form of the π-bonding interference function was constructed to insure that some π bonding would be present to stabilize the π-bonded-chain reconstruction of the Si(111) surface. All other calculated properties of surfaces therefore represent predictions of our model potential. We present here the results using our potential on the Si(100) dimer reconstruction, the Si(111) π-bond-chain model, the $\sqrt{3}\times\sqrt{3}$ adatom configurations on Si(111), and the 7×7 reconstruction of Si(111).

There has long been disagreement over the experimental structure of the Si(100) surface. Various experimental methods such as low-energy electron diffraction and He-atom diffraction[48] have been ineffective in conclusively determining the structure, and have led to various proposals for the surface cell. Recently Hamers *et al.*[49] have helped to clarify the issue using scanning tunneling microscopy. They concluded that dimers are the primary type of reconstruction that contribute to the surface. Far from defects, the surface forms 2×1 symmetric dimers. [In the presence of a defect these dimers tend to buckle and form $p(2\times2)$ and $c(4\times2)$ structures.]

We have studied the Si(100) 2×1 structure by performing calculations on a system of five layers of 16 atoms/layer, with the layers being perpendicular to the Si [001] direction. Initially, all the atoms were placed in a structure corresponding to a perfect crystal, and the energy was calculated; this gives the energy of a perfect unreconstructed surface. Then the structure was distorted toward that of the 2×1 dimer reconstruction, and the top three layers were relaxed by steepest-descent energy minimization, keeping the bottom two layers fixed. The system adopted a 2×1 dimer structure, which is a local minimum (and most likely the global minimum) on the potential surface for the system. The reconstructed surface had an energy that was 1.60 eV/dimer lower than that of the perfect unreconstructed surface. We have summarized the results and compared with other models in Table VI. Our results are similar to those of DFT-LDA and of all the other potential functions tested. This is by far the easiest of the reconstructions to describe correctly, since most potentials will favor the formation of new bonds in the dimer structure.

At temperatures below 380 °C the Si(111) surface exhibits a (2×1) reconstruction. The most accepted model for this reconstruction is the π-bonded-chain model of Pandey.[39] This reconstruction is a stringent test of our potential's ability to model π-bonding situations. In this case we use a slab, periodic in two dimensions, having a perfect 111 surface on both faces and eight layers thick.

TABLE VI. Si(100) 2×1 dimer reconstruction. The relaxation energy per dimer reported here is the energy of the perfect unreconstructed surface minus the energy of the 2×1 structure, divided by the number of dimers. R_{dimer} is the separation of the dimers in the equilibrium structure. The Yin and Cohen (YC) and Pandey references are density functional calculations.

Method	R_{dimer} (Å)	Relaxation energy per dimer (eV/dimer)
YC (Ref. 46)	2.25	1.70
Pandey (Ref. 36)	2.22	2.06
SW	2.41	1.68
TER2	2.31	2.40
BH2	2.42	1.73
Present	2.36	1.60

We calculated the surface energy[50] of the perfect unreconstructed surface by calculating the energy of this slab, subtracting the energy of the same number of bulk atoms, and dividing by 2 (since we have two surfaces). We found the surface energy per unit area of the perfect unreconstructed surface to be 0.091 eV/Å^2. The top two layers of one face of the slab were moved to positions near the struture of the π-bonded-chain model of Pandey and a steepest-descent energy minimization was carried out, keeping the bottom four layers fixed and allowing the top four layers to relax. The system settled into a local minimum with a structure similar to the Pandey model. The energy of this slab was 0.021 eV/Å^2 less than the energy of the unreconstructed slab. Thus the surface energy of the 2×1 π-bond-chain reconstruction is 0.070 eV/Å^2. This is consistent with the experimental observation of the spontaneous reconstruction at low temperatures. Northrup and Cohen reported a DFT-LDA energy of -0.37 eV/atom relative to the perfect surface.[54] If one assumes that they are considering the two top layers, which have positions that cannot be related to bulk lattice sites, as surface layers, then his figure corresponds to 0.029 eV/Å^2 lower than the perfectly cleaved surface, which is close to our result.

Table VII compares the results for the present potential, the TER2 potential, and the DFT. The TER2 potential has a local minimum at the Pandey structure but predicts the reconstructed surface to be higher in energy than the unreconstructed surface, rather than lower. The

TABLE VII. Si(111) π-chain reconstruction. R_{chain} is the distance between silicon atoms in the π bonded chain running along the top of the surface. NC refers to the density functional results of Northrup and Cohen. The surface energy shown is the surface energy of the reconstructed π chain minus the surface energy of the perfect Si(111) surface.

Method	R_{chain} (Å)	Surface $E_{\pi\text{ chain}}-E_{(111)}$ (eV/Å^2)
NC (Ref. 54)		-0.029
TER2	2.28	$+0.010$
Present	2.21	-0.021

TABLE VIII. Si(111) T_4 and H_3 adatom geometries and energies. In the notation for the atom-atom distances, 1=adatom, 2=first-layer atom, and 3=second-layer atom. Refer to Northrup (Ref. 55) for further explanation of notation.

	T_4		H_3			
Method	R_{1-3a} (Å)	R_{1-2} (Å)	R_{1-2} (Å)	R_{1-3} (Å)	$E(T_4)$ (eV/adatom)	$E(H_3)$ (eV/adatom)
Northrup (Ref. 55)	2.49	2.49	2.55	3.05	−0.84	−0.20
SW (Ref. 31)	2.84	2.89	3.28	3.84	+2.16	+1.05
TER2	2.39	2.42	2.40	3.09	−0.20	−0.42
BH2	2.56	2.61	2.51	3.07	+0.89	+0.47
Present	2.38	2.51	2.43	2.64	−0.03	−0.25

BH2 potential does not have a local minimum at the chain structure. The results for TER2 and BH2 are a reflection of the fact that these potentials do not correctly describe π bonding. As noted above, the π interference function of the present potential was constructed in such a way as to insure that π bonding would contribute to stabilizing this surface structure.

Adatoms on the Si(111) 7×7 surface were observed by Binning *et al.*[51] and are thought to play an important role in its reconstruction. The dimer–adatom–stacking-fault (DAS) model proposed by Takayanagi *et al.*[52] has become the most generally accepted model for this reconstruction. A unit cell of the DAS model contains 12 silicon atoms in T_4 adatom positions. To be confident that a potential might be useful for studying the 7×7 reconstruction it should model T_4 and H_3 adatom geometries and energies correctly. These adatom geometries involve large bond-angle distortions from the ideal tetrahedral angle. There are two aspects of the adatom energies that are important for a potential to model correctly. First, the adatoms need to lower the surface energy (i.e., the energy that is takes to transfer one atom from a bulk lattice site to an adatom position should be negative.) Second, the T_4 adatom geometry should be lower in energy than the H_3 geometry. It has been found by Li *et al.*[53] and Khor and Das Sarma[31] that the SW and TER2 potentials both predict the H_3 configuration to be lower in energy than T_4. In this respect, these two potentials are deficient. The TER2 potential exhibited a lowering of the total surface energy for both adatoms' configurations. Li *et al.* showed that, even with the problem of the relative T_4 and H_3 energies, the TER2 potential was very useful for predicting the energy and vibrational spectra of the Si(111) 7×7 reconstruction. Our potential does a reasonable job for both the T_4 and H_3 configurations in predicting a lowering of the surface energy (see Table VIII). Unfortunately, our potential is similar to Tersoff's in having a H_3 geometry lower in energy. Given the work of Li *et al.* and the fact that our potential models the elastic constants for the diamond lattice very well, we believe that the present potential would still be extremely useful in studying the 7×7 reconstruction. We have performed preliminary calculations with Tersoff's TER3 (Ref. 22) potential and noticed that the adatoms actually raise, instead of lower, the (111) surface energy. This may demonstrate a limitation of the functional form that he is using, in that he is finding it difficult to model both the surface and bulk properties simultaneously.

The DAS model of the 7×7 reconstructions of Si(111) involves the formation of both adatoms and dimer chains. Experimentally, the 7×7 surface is a structure formed by annealing either the 1×1 or 2×1 surface at temperatures as low as 300 °C. If the high-temperature 7×7 surface is cooled very slowly, with annealing, it remains in this structure indefinitely. We have performed energy minimizations of a 7×7 surface cell containing 249 atoms, 102 of which are reconstructed surface atoms, making up three layers. The 102 surface atoms were allowed to relax and the 7×7 structure was found to be a local minimum. The surface energy with the present model was 0.102 eV/Å^2, which is higher than the 0.091 eV/Å^2 of a perfect Si(111) surface. This is an upper bound to our potential's 7×7 surface energy, since it would decrease if more layers were allowed to relax. We did a limited relaxation of the next layer (the first bulk layer) and found the surface energy decreased to 0.100 eV/Å^2. More extensive calculations were not feasible with our present computational resources. The fact that a local minimum is found is encouraging, and shows that this potential is applicable to studies of the 7×7 reconstruction or adsorption upon this surface. Experimental relative surface energies of the 7×7 and perfect Si(111) surfaces are not known. Since the 7×7 structure forms only at high temperature, it is conceivable that the real 7×7 structure is a local minimum, rather than a global minimum, on the potential-energy surface, and that it is higher in energy than the perfect Si(111) surface.

IV. CONCLUSION

The need to model covalent systems in a wide range of bonding situations is evident. Much effort has recently been devoted to silicon, and has been applied in two directions. First, potentials have been developed that attempt to model silicon in as many bonding situations as possible. Secondly, specific models have been developed that apply only to limited situations.

We have taken the first approach and used a functional form, much like Tersoff's, that includes environment dependence of the bondings in the two-body potential. This avoids the problem of expanding the potential in a series of many-body interactions that become increasingly difficult to represent and promise little hope of convergence. By modeling small clusters we found that a sepa-

ration of the interactions into π- and σ-bonding terms was physically reasonable and in practice necessary. The extra flexibility has allowed the present potential to accurately model a wider range of silicon systems than any other potential to date. In addition, based upon the type of local minima on the potential-energy surface, we have provided evidence that Tersoff's and our potential are qualitatively different from the potentials of Stillinger and Weber and Biswas and Hamann. Our potential goes beyond the Tersoff(II) potential, in being able to more effectively represent π bonding in small clusters and surfaces.

The procedure of using both *ab initio* cluster information and bulk experimental data to determine a potential should be applicable to a wide range of materials. We believe the general Tersoff form to be a promising way of representing many-body interactions for covalent systems, especially when combined with the separation of the π and σ interactions. We believe that many other systems, such as carbon, could be modeled just as effectively as silicon.

ACKNOWLEDGMENTS

We would like to thank the National Science Foundation (NSF) for its support under Grant No. CHE-84-10701, and the San Diego Supercomputer Center for providing computational resources. The early stages of this work were partially supported by the Stanford University Center for Materials Research, funded by the NSF. In the later stages, one of us (B.B.) received partial support, under Grant No. P200A80071, from the U.S. Department of Education. We appreciate discussions with Dr. Richard Messmer and Dr. Krishnan Ragavachari and reports of their work prior to publication. We appreciate discussions with Birgit Koehler concerning experimental silicon surfaces. We also thank Dr. William Busing of Oak Ridge National Laboratories for providing us with the WMIN program.

[1]K. Ragavachari, J. Chem. Phys. **83**, 3520 (1985).
[2]K. Ragavachari and V. Logovinsky, Phys. Rev. Lett. **55**, 2853 (1985).
[33]K. Ragavachari, J. Chem. Phys. **84**, 5672 (1986).
[4]K. Ragavachari and C. M. Rohlfing, Chem. Phys. Lett. **143**, 428 (1988).
[5]K. Ragavachari and C. M. Rohlfing, J. Chem. Phys. **89**, 2219 (1988).
[6]G. Pacchioni and J. Koutecký, J. Chem. Phys. **84**, 3301 (1986).
[7]C. H. Patterson and R. P. Messmer (unpublished report).
[8]P. Ballone, W. Andreoni, R. Car, and M. Parrinello, Phys. Rev. Lett. **60**, 271 (1988).
[9]D. Tomańek and M. A. Schlüter, Phys. Rev. B **36**, 1208 (1987).
[10]J. Chelikowsky, Phys. Rev. Lett. **60**, 2669 (1988).
[11]P. N. Keating, Phys. Rev. **145**, 637 (1966).
[12]E. Pearson, T. Takai, T. Halicioglu, and W. A. Tiller, J. Crystal Growth **70**, 33 (1984).
[13]T. Takai, T. Halicioglu, and W. A. Tiller, Scripta Metall. **19**, 709 (1985).
[14]F. Stillinger and T. A. Weber, Phys. Rev. B **31**, 5262 (1985).
[15]B. W. Dodson, Phys. Rev. B **33**, 7361 (1986).
[16]K. E. Khor and S. Das Sarma, Phys. Rev. B **36**, 7733 (1987).
[17]B. P. Fueston, R. K. Kalia, and P. Vashishta, Phys. Rev. B **35**, 6222 (1987).
[18]B. P. Fueston, R. K. Kalia, and P. Vashishta, Phys. Rev. B **37**, 6297 (1988).
[19]E. Blaisten-Barojas and D. Levesque, Phys. Rev. B **34**, 3910 (1986).
[20]J. Tersoff, Phys. Rev. Lett. **56**, 632 (1986).
[21]J. Tersoff, Phys. Rev. B **37**, 6991 (1988).
[22]J. Tersoff, Phys. Rev. B **38**, 9902 (1988).
[23]R. Biswas and D. R. Hamann, Phys. Rev. Lett. **55**, 2001 (1985).
[24]R. Biswas and D. R. Hamann, Phys. Rev. B **36**, 6434 (1987).
[25]B. W. Dodson, Phys. Rev. B **35**, 2795 (1987).
[26]D. W. Brenner and B. J. Garrison, Phys. Rev. B **34**, 1304 (1986).
[27]J. Chelikowsky, J. C. Phillips, M. Kamal, and M. Strauss, Phys. Rev. Lett. **62**, 292 (1989).
[28]H. Wang and R. P. Messmer (unpublished report).
[29]J. Chelikowsky and J. C. Phillips, Phys. Rev. Lett. **63**, 1653 (1989).
[30]K. E. Khor and S. Das Sarma, Phys. Rev. B **38**, 3318 (1988).
[31]K. E. Khor and S. Das Sarma, Phys. Rev. B **39**, 1188 (1989).
[32]M. I. Baskes, Phys. Rev. Lett. **59**, 2666 (1987).
[33]M. S. Daw and M. I. Baskes, Phys. Rev. Lett. **50**, 1285 (1983).
[34]M. S. Daw and M. I. Baskes, Phys. Rev. B **29**, 6443 (1984).
[35]The cohesive energies reported here are slightly different from those reported by Ragavachari in some of his papers. He included a correction for zero-point vibrations, and we have used only the *ab initio* energies at the local minima without this correction.
[36]K. C. Pandey, Phys. Rev. Lett. **49**, 223 (1982).
[37]G. C. Abell, Phys. Rev. B **31**, 6184 (1985).
[38]The lattice constant is from J. Donohue, *The Structures of Elements* (Wiley, New York, 1974). The cohesive energy is from L. Brewer, Lawrence Berkeley Laboratory Report No. LBL-3720 (unpublished). The phonon frequencies are from G. Dolling, *Inelastic Scattering of Neutrons in Solids and Liquids* (Unipub, New York, 1963), Vol. II, p. 42. The bulk modulus is from H. J. McSkimin, J. Appl. Phys. **24**, 988 (1953).
[39]K. C. Pandey, Phys. Rev. B **47**, 1913 (1981).
[40]L. A. Bloomfield, R. R. Freeman, and W. L. Brown, Phys. Rev. Lett. **54**, 2246 (1985).
[41]G. A. Baraff and M. Schlüter, Phys. Rev. B **30**, 3460 (1984).
[42]Y. Bar-Yam and J. D. Joannopolous, Phys. Rev. Lett. **52**, 1129 (1984).
[43]R. Car, P. J. Kelly, A. Oshiyama, and S. T. Pantelides, Phys. Rev. Lett. **52**, 1814 (1984).
[44]R. Car, P. J. Kelly, A. Oshiyama, and S. T. Pantelides, Phys. Rev. Lett. **54**, 360 (1985).
[45]M. T. Yin and M. L. Cohen, Phys. Rev. Lett. **45**, 1004 (1980).
[46]M. T. Yin and M. L. Cohen, Phys. Rev. B **26**, 5668 (1982).
[47]M. T. Yin and M. L. Cohen, Phys. Rev. B **29**, 6996 (1984).
[48]M. J. Cardillo and G. E. Becker, Phys. Rev. B **21**, 1497 (1980).
[49]R. J. Hamers, R. M. Tromp, and J. E. Demuth, Phys. Rev. B **34**, 5343 (1986).

[50]The surface energy is defined as the total energy of a system of N atoms, having a surface, minus N times the cohesive energy per atom in the bulk.
[51]G. Binnig, H. Rohrer, C. Gerber, and E. Weibel, Phys. Rev. Lett. **50**, 120 (1983).
[52]K. Takayanagi, Y. Tanishiro, M. Takahashi, and S. Takahashi, J. Vac. Sci. Technol. A **3**, 1502 (1985).
[53]X. P. Li, G. Chen, P. B. Allen, and J. Q. Broughton, Phys. Rev. B **38**, 3331 (1988).
[54]J. E. Northrup and M. L. Cohen, Phys. Rev. Lett. **49**, 1349 (1982).
[55]J. E. Northrup, Phys. Rev. Lett. **57**, 154 (1986).